

## Temperature Measurement by a Nanoscale Electron Probe Using Energy Gain and Loss Spectroscopy

Juan Carlos Idrobo,<sup>1,\*</sup> Andrew R. Lupini,<sup>2,†</sup> Tianli Feng,<sup>3,2</sup> Raymond R. Unocic,<sup>1</sup> Franklin S. Walden,<sup>4</sup> Daniel S. Gardiner,<sup>4</sup> Tracy C. Lovejoy,<sup>5</sup> Niklas Dellby,<sup>5</sup> Sokrates T. Pantelides,<sup>3,2</sup> and Ondrej L. Krivanek<sup>5</sup>

<sup>1</sup>Center for Nanophase Materials Sciences, Oak Ridge National Laboratory, Oak Ridge, Tennessee 37831, USA

<sup>2</sup>Materials Science and Technology Division, Oak Ridge National Laboratory, Oak Ridge, Tennessee 37831, USA

<sup>3</sup>Department of Physics and Astronomy and Department of Electrical Engineering and Computer Science, Vanderbilt University, Nashville, Tennessee 37235, USA

<sup>4</sup>Protochips Company, 3800 Gateway Centre Boulevard, Suite 306, Morrisville, North Carolina 27560, USA

<sup>5</sup>Nion Company, 11511 NE 118th Street, Kirkland, Washington 98034, USA



(Received 23 October 2017; revised manuscript received 12 January 2018; published 2 March 2018)

Heat dissipation in integrated nanoscale devices is a major issue that requires the development of nanoscale temperature probes. Here, we report the implementation of a method that combines electron energy gain and loss spectroscopy to provide a direct measurement of the local temperature in the nanoenvironment. Loss and gain peaks corresponding to an optical-phonon mode in boron nitride were measured from room temperature to  $\sim 1600$  K. Both loss and gain peaks exhibit a shift towards lower energies as the sample is heated up. First-principles calculations of the temperature-induced phonon frequency shifts provide insights into the origin of this effect and confirm the experimental data. The experiments and theory presented here open the doors to the study of anharmonic effects in materials by directly probing phonons in the electron microscope.

DOI: [10.1103/PhysRevLett.120.095901](https://doi.org/10.1103/PhysRevLett.120.095901)

Thermal management is essential for the microelectronics industry to improve the energy efficiency of electronic components [1], meaning that there is an urgent need to be able to map the local temperature of individual microelectronics devices. Local temperature measurements with nanoscale spatial resolution have recently been achieved by tracking the energy shifts of bulk plasmons as functions of temperature in scanning transmission electron microscopy (STEM) [2]. This concept dates to the mid 1950s [3], when it was pointed out that the energy of a bulk plasmon depends on the temperature through changes in volume and the associated changes in electron density. Another concept, which originated in the 1960s, determines the local temperature by measuring the energy gains of a fast electron beam interacting with the phonons in a material [4–6], with the gains first observed by Boersch *et al.* [4] at micrometer spatial resolution. However, despite the fact that monochromators have been available in electron microscopes for several decades, it is only in the last few years that it has become possible to resolve phonons and to study them with nanometer spatial resolution [7–10].

In this Letter, we take advantage of the ability of a modern monochromated aberration-corrected STEM system to record energy-gain spectra to determine the temperature of a material by measuring the ratio between the gain and loss phonon peaks in the electron energy spectrum. The loss and gain peaks from hexagonal boron nitride (*h*-BN) nanoflakes, corresponding to an optical phonon mode,

were measured over a temperature range from room temperature to  $\sim 1600$  K. We find that both peaks present a red shift (towards lower energies) as the sample is heated up, with a linear behavior over the temperature range used here. First-principles calculations reveal that the redshift is due to a combination of lattice thermal expansion and anharmonic phonon scattering, with the latter being the dominant factor to reduce the energy of the optical phonon as the temperature of the sample increases. The gain peak exhibits a clear increase of intensity as a function of temperature, in accordance with the occupation probability of the phonon energy state. The spectroscopy presented in this study shows that by detecting both gain and loss peaks, the local temperature of a material can be obtained from purely statistical principles.

The *h*-BN nanoflakes were dispersed on a holey carbon film as shown in the *Z*-contrast STEM image in Fig. 1. The incident electron probe was positioned in a hole, near to the center of an agglomeration of *h*-BN nanoflakes. The spectra were acquired in an aloof configuration, with the beam in free space, at a distance from the *h*-BN nanoflakes of about 50 nm.

Figure 2 shows the gain and loss phonon peaks of *h*-BN obtained over a temperature range from 323 to 1586 K, with an average temperature step of 55 K, using 5 seconds acquisition time. Each plotted spectrum line is the average of ten different spectra. All the spectra were normalized for display such that the intensity of the loss phonon peak for

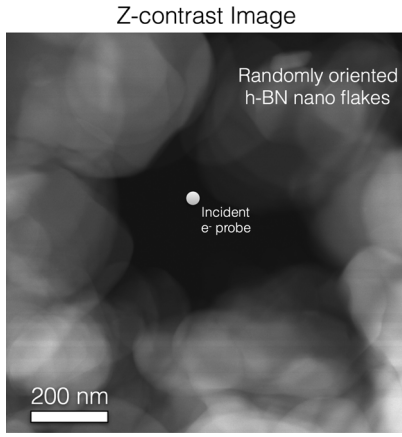


FIG. 1. Z-contrast image of the studied *h*-BN nanoflakes. The sub-nm-sized incident electron beam is in vacuum about 50 nm from the closest particle, allowing for aloof spectroscopy. The gray circle shows the approximate incident electron beam position.

each temperature was equal to 1. Further details of the experiments can be found in the STEM-EELS experiments section in Ref. [11].

The loss peak shown in Figs. 2(a) and 2(c) corresponds to a high-energy *h*-BN optical-phonon mode, which is located at 186.5 meV when measured at room temperature. Moreover, it can be seen that as the temperature of the sample increases, the energy-gain peak becomes visible over the background noise above  $\sim 473$  K and then increases with temperature. The increased intensity of the gain peak with temperature is better appreciated after the background has been subtracted, as shown in Fig. 2(b). The gain peak intensity ranges from 1% to 27% of the loss peak intensity.

The change of intensity of the gain peak with temperature allows the direct measurement of the temperature of the *h*-BN nanoflakes using the principle of detailed balance [21]. This principle of statistical physics relates the probabilities of a transition from a lower to a higher energy state ( $P_L$ , loss mode) and its reverse ( $P_G$ , gain mode) by the Boltzmann factor,  $\exp(-E_{ph}/kT)$ , as  $P_G = \exp(-E_{ph}/kT)P_L$ , where  $E_{ph}$  is the energy of the phonon,  $k$  is the Boltzmann constant, and  $T$  is the temperature of the sample.

Figure 3 shows the experimental gain and loss peaks  $P_G/P_L$  (same as  $I_{Gain}/I_{Loss}$ ) ratios compared with the Boltzmann factor, which was obtained using the experimentally measured phonon energy for the reported nominal temperature from the microelectromechanical system (MEMS) chip. There is clearly a good match obtained between the experimental  $P_G/P_L$  ratios and the calculated Boltzmann factor, as expected from the principle of detailed balance.

The inset of Fig. 3 visually indicates the accuracy of the temperature obtained by the principle of detailed balance  $T_{GL}$  compared with the nominal temperature reported by

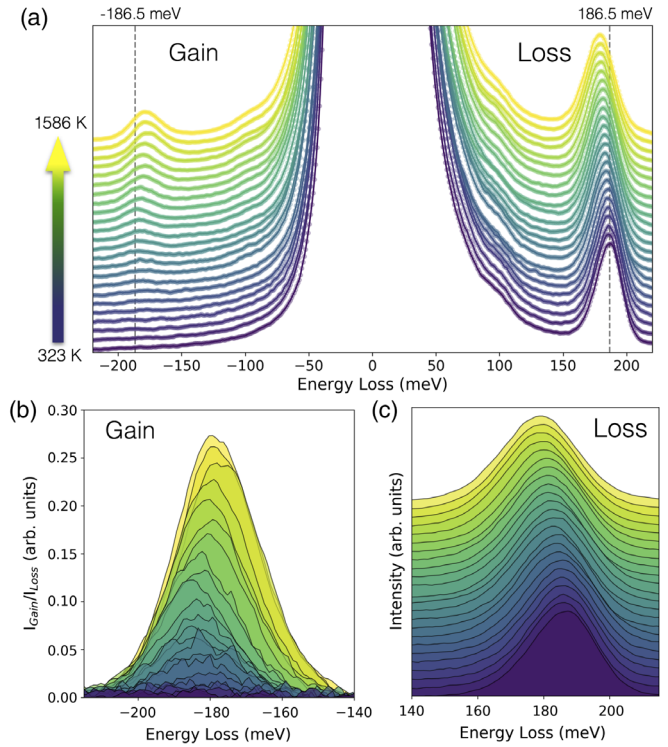


FIG. 2. Electron energy-loss and energy-gain spectra of *h*-BN as a function of temperature. (a) Spectra acquired as a function of temperature from 323 to 1586 K, with average increment steps of 55 K. (b) Electron energy-gain spectra shown in (a) after the background has been subtracted. The intensity of each gain peak ( $I_{Gain}$ ) has been normalized with the intensity of the loss peak ( $I_{Loss}$ ) obtained at the same nominal temperature. (c) Electron energy-loss peaks shown in (a). The loss peak corresponds to a *h*-BN high-energy optical-phonon mode. Notice that the phonon peaks shift in energy as a function of temperature. The spectra in (a) and (c) have been vertically shifted for illustration purposes.

the device, which has an accuracy of 5%. The precision in the temperature measurements depends linearly on the precision in determining the phonon energy and the ratio of the gain and loss peaks. The scatter in the  $P_G/P_L$  ratio is the main source of error in the spectroscopy method. For lower energy phonons, such as those reported in  $\text{SiO}_2$  [7], the intensity of  $P_G$  increases, resulting in a reduction of the scatter in the  $P_G/P_L$  ratio, which should improve the precision of the method at the low end of the temperature range.

Figure 2 reveals that both gain and loss phonon peaks shift in energy as the temperature increases. The temperature dependence of the *h*-BN phonon mode parameters, energy and line width (or full-width half-maximum) are plotted in Figs. 4(a) and 4(b), respectively. The energy shift of the *h*-BN phonon mode is well described by a linear fit, with a fitted slope of  $-6.08 \mu\text{eV/K}$ . Additionally, a measurable increase of the line width of the phonon loss peak is observed with temperature [Fig. 4(b)]. The line width of the loss phonon mode increases by about 2.4 meV,

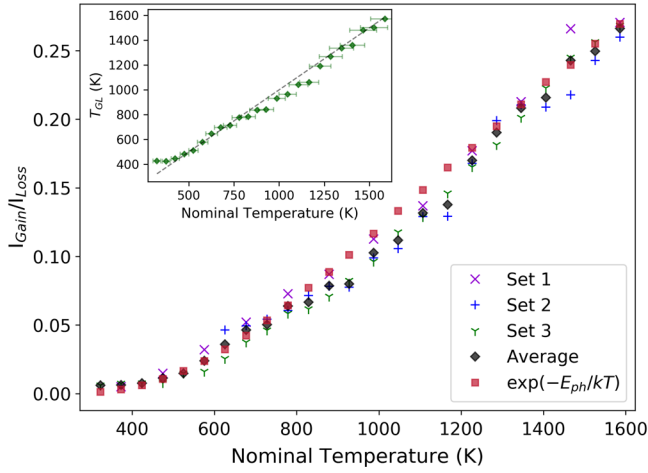


FIG. 3. Gain and loss phonon peak intensity ratios. Gain and loss phonon peak intensity ( $I_{\text{Gain}}/I_{\text{Loss}}$ ) ratios of three different sets of measurements performed at different times (and the respective average) compared with the Boltzmann factor  $\exp(-E_{\text{ph}}/kT)$ . The experimentally measured phonon energy, as well as the reported nominal temperature  $T$  from the MEMS heater microchip device are used in the calculation of the Boltzmann factor data points. The inset shows the temperature obtained by the principle of detailed balance  $T_{GL}$  against the nominal temperature. The error bars indicate the 5% accuracy of the MEMS device temperature.

from 14.3 meV at 323 K to 16.7 meV at 1586 K. Although the noise in the data for the gain peak does not allow us to determine a clear trend with temperature, its mean line width from 323 to 1586 K is 16.0 meV with a standard deviation of 0.7 meV.

In order to understand the origin of the phonon energy shift, first-principles calculations based in density functional theory and *ab initio* molecular dynamics were performed. Details of the calculations can be found in the first-principles calculations section in Ref. [11]. The energy shift at temperatures originates from a combination of lattice thermal expansion and anharmonic phonon scattering. The lattice thermal expansion increases the energy of the phonon (*h*-BN has negative thermal expansion in plane); however, as can be seen in the inset of Fig. 4(a), the anharmonic phonon scattering dominates, resulting in a decrease of the phonon energy with temperature. Our experimental and theoretical results are in agreement with previous work [16,22,23] and highlight the sensitivity of monochromated high-energy resolution electron spectroscopy to capture the phonon behavior of materials with high spatial resolution.

As shown in Fig. 4(a), the energy of the phonon mode varies with temperature and can thus be used to measure the local temperature, in much the same way as for plasmon energy shifts [5]. However, relying on energy shifts requires an empirical calibration of how the phonon mode softens (shifts in energy) with temperature, unlike the parameter-free method relying on detailed balance.

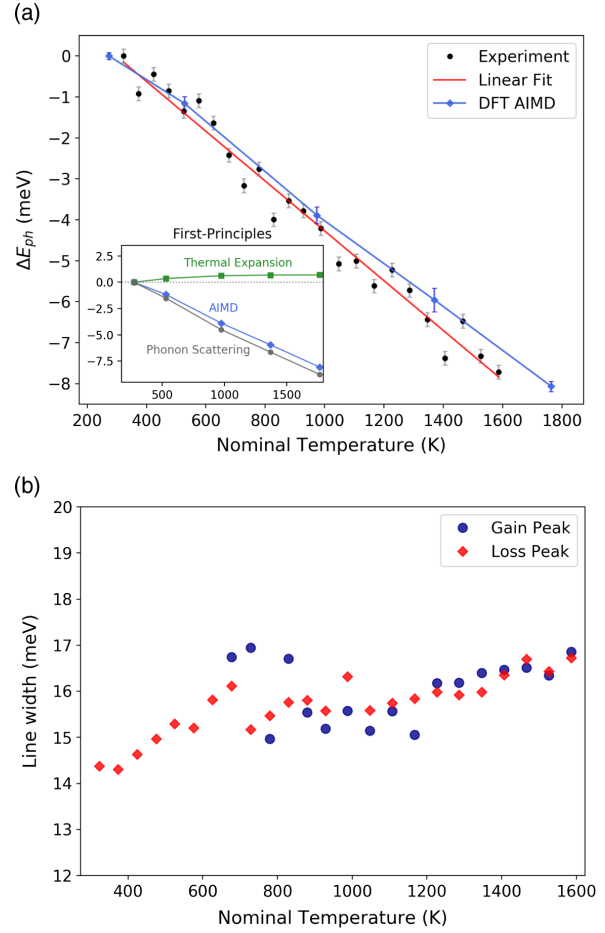


FIG. 4. Temperature dependence of the *h*-BN phonon mode parameters. (a) The energy shift of the *h*-BN phonon mode is well described by a linear behavior, with a calculated slope of the energy shift of  $-6.08 \mu\text{eV}/\text{K}$ . (b) The line width of the phonon loss peak is observed to increase with temperature by about 2.4 meV, from 14.3 meV at 323 K to 16.7 meV at 1586 K. The variation in the gain data does not allow us to obtain a clear trend of its line width with temperature.

Here we have presented the first measurements of the ratio between gain and loss phonon peaks as a function of temperature using a nanoscale probe. The experiments in this study show that by detecting gain peaks, the local temperature of a material can be obtained directly, based purely on statistical principles, and indirectly (using empirical fits, as done previously by analyzing the changes in contrast of high-angle annular dark field images [24] or from parallel-beam electron diffraction patterns [25]). The experiments, combined with first-principles calculations, show that direct measurements of the thermal expansion coefficients and the phonon scattering behavior are accessible with far better spatial resolution than optical methods such as Raman spectroscopy, or neutron scattering, which rely on larger volumes. Thus, the anharmonic behavior of materials due to confinement effects (particle size) and the influence of localized defects, may now be open for study

with the electron microscope in penetrating or aloof beam mode conditions, allowing a choice between even higher spatial resolution or low beam damage. In the same way as recently demonstrated with plasmonic excitations [2], the energy-gain spectroscopy technique presented here constitutes the foundation of a possible methodology to measure the temperature of working microelectronic devices with high spatial resolution.

This research was supported by the Center for Nanophase Materials Sciences, which is a Department of Energy Office of Science User Facility (J. C. I. and R. R. U.), and by the Materials Sciences and Engineering Division Office of Basic Energy Sciences, U.S. Department of Energy (A. R. L.). This research used resources of the National Energy Research Scientific Computing Center, which is supported by the Office of Science of the U.S. Department of Energy under Contract No. DE-AC02-05CH11231, and instrumentation within ORNL's Materials Characterization Core provided by UT-Battelle, LLC under Contract No. DE-AC05-00OR22725 with the U.S. Department of Energy. This work used the Extreme Science and Engineering Discovery Environment (XSEDE). Theoretical work at Vanderbilt University was supported by DOE Award No. DE-FG02-09ER46554 and by the McMinn Endowment (T. L. F. and S. T. P.). J. C. I. acknowledges Michael Manley at ORNL for useful discussions, and Hye Jung Chang, Hans Christen, Robert Klie, Karren More, and Ján Rusz for input with the manuscript.

---

\*idrobojc@ornl.gov

†arl1000@ornl.gov

- [1] E. Pop, S. Sinha, and K. E. Goodson, *Proc. IEEE* **94**, 1587 (2006).
- [2] M. Mecklenburg, W. H. Hubbard, E. R. White, R. Dhall, S. B. Cronin, S. Aloni, and C. Regan, *Science* **347**, 629 (2015).
- [3] H. Watanabe, *J. Phys. Soc. Jpn.* **11**, 112 (1956).
- [4] H. Boersch, J. Geiger, and W. Stickel, *Phys. Rev. Lett.* **17**, 379 (1966).
- [5] A. Howie, *Inst. Phys. Conf. Ser.* **161**, 311 (1999).
- [6] F. J. García de Abajo and M. Kociak, *New J. Phys.* **10**, 073035 (2008).
- [7] O. L. Krivanek *et al.*, *Nature (London)* **514**, 209 (2014).
- [8] P. Rez, T. Aoki, K. March, D. Gur, O. L. Krivanek, N. Dellby, T. C. Lovejoy, S. G. Wolf, and H. Cohen, *Nat. Commun.* **7**, 10945 (2016).
- [9] C. Dwyer, T. Aoki, P. Rez, S. L. Y. Chang, T. C. Lovejoy, and O. L. Krivanek, *Phys. Rev. Lett.* **117**, 256101 (2016).
- [10] M. J. Lagos, A. Trüger, U. Hohenester, and P. E. Batson, *Nature (London)* **543**, 529 (2017).
- [11] See Supplemental Material <http://link.aps.org/supplemental/10.1103/PhysRevLett.120.095901> for a description of the experimental details and first-principles calculations, which includes Refs. [12–20].
- [12] O. L. Krivanek, T. C. Lovejoy, N. Dellby, and R. W. Carpenter, *Microscopy* **62**, 3 (2013).
- [13] G. Kresse and J. Hafner, *Phys. Rev. B* **47**, 558 (1993).
- [14] G. Kresse and J. Furthmüller, *Phys. Rev. B* **54**, 11169 (1996).
- [15] G. Kresse, and J. Furthmüller, *Comput. Mater. Sci.* **6**, 15 (1996).
- [16] G. J. Exarhos and J. W. Schaaf, *J. Appl. Phys.* **69**, 2543 (1991).
- [17] A. Togo and I. Tanaka, *Scr. Mater.* **108**, 1 (2015).
- [18] N. de Koker, *Phys. Rev. Lett.* **103**, 125902 (2009).
- [19] T. L. Feng and X. L. Ruan, *J. Appl. Phys.* **117**, 195102 (2015).
- [20] U. Argaman, E. Eidelstein, O. Levy, and G. Makov, *Phys. Rev. B* **94**, 174305 (2016).
- [21] G. L. Squires, *Thermal Neutron Scattering*, 3rd ed. (Cambridge University Press, Cambridge, 2012).
- [22] B. Yates, M. J. Overy, and O. Pirgon, *Physica magazine* **32**, 847 (1975).
- [23] R. Cuscó, B. Gil, G. Cassabois, and L. Artús, *Phys. Rev. B* **94**, 155435 (2016).
- [24] M. Libera, J. A. Ott, and K. Sianghaew, *Ultramicroscopy* **63**, 81 (1996).
- [25] F. Niekiel, S. M. Kraschewski, J. Müller, B. Butz, and E. Spiecker, *Ultramicroscopy* **176**, 161 (2017).

# Supplemental Material: Temperature Measurement by a Nanoscale Electron Probe Using Energy Gain and Loss Spectroscopy

Juan Carlos Idrobo,<sup>1</sup> Andrew R. Lupini,<sup>2</sup> Tianli Feng,<sup>3</sup> Raymond R.  
Unocic,<sup>1</sup> Franklin S. Walden,<sup>4</sup> Daniel S. Gardiner,<sup>4</sup> Tracy C. Lovejoy,<sup>5</sup>  
Niklas Dellby,<sup>5</sup> Sokrates T. Pantelides,<sup>3</sup> and Ondrej L. Krivanek<sup>5</sup>

<sup>1</sup>*Center for Nanophase Materials Sciences,  
Oak Ridge National Laboratory, Oak Ridge,  
TN 37831, United States of America\**

<sup>2</sup>*Materials Science and Technology Division,  
Oak Ridge National Laboratory, Oak Ridge,  
TN 37831, United States of America<sup>†</sup>*

<sup>3</sup>*Department of Physics and Astronomy and Department  
of Electrical Engineering and Computer Science,  
Vanderbilt University, Nashville, TN 37235, United States of America*

<sup>4</sup>*Protochips Company, 3800 Gateway Centre Blvd,  
Suite 306, Morrisville, NC 27560, United States of America*

<sup>5</sup>*Nion Company, 11511 NE 118th St, Kirkland,  
WA 98034, United States of America*

## STEM-EELS experiments

The experiments were performed in a monochromated and aberration-corrected STEM Nion HERMES 100, equipped with a cold field emission electron source and a fifth order aberration corrector, operating at 60 kV accelerating voltage [1]. EEL spectra were collected using a Nion prototype spectrometer, with 1.3 meV/channel dispersion. The spectra were acquired with an energy resolution of about 14 meV, as measured by the FWHM of the zero-loss peak (ZLP) at room temperature. The convergence semi-angle for the incident probe and the EELS collection semi-angle were 15 mrad and 21 mrad, respectively. The Z-contrast images were collected using an annular detector with an inner angle of roughly 86 mrad.

To accurately measure the energy peak position of the gain and loss phonon peaks the experiments were repeated acquiring ten different spectra with an acquisition time of 50 ms per spectrum at each temperature. The short acquisition time allowed simultaneous collection of the ZLP and the phonon modes (which have a 3 orders of magnitude smaller intensity than the ZLP) without saturation of the spectrometer camera. The energy of the phonon modes obtained with the short acquisition time were used to calibrate the spectra shown in Fig. 2, used in Set 2 of Fig. 3 and in Fig. 4a of the main manuscript.

The heating of the sample was performed using an implementation of Protochips Fusion<sup>TM</sup>, which was integrated in the Nion microscope. It utilizes MEMS based microchip heating devices to control the sample's temperature by resistively heating a thin film SiC membrane using a Keithley 2636B source meter. The temperature of the chip is measured with a thermal camera under vacuum conditions up to 1173 K (900 °C). For experiments performed at higher temperatures than 1173 K, the reported nominal temperature in the chip is extrapolated from the calibration measurements of current vs temperature.

## First-principles calculations

The first-principles density functional theory (DFT) calculations are performed using the projector augmented wave (PAW) method with the local density approximation (LDA) as implemented in the VASP package [2–4]. The plane wave cutoff energy is 550 eV. In the static relaxation for a unit cell with a  $13 \times 13 \times 9$  k-mesh, the energy and force convergence

criteria are  $10^{-8}$  eV and  $10^{-6}$  eV/Å, respectively. The obtained lattice constants = 2.490 and = 6.451 Å agree well with experimental values = 2.504 and = 6.660 Å [5].

The quasi-harmonic phonon dispersions at given lattice constants are calculated via the PHONOPY package [6] with a  $4 \times 4 \times 2$  supercell and  $5 \times 5 \times 3$  k-mesh. The *ab initio* molecular dynamics (AIMD) simulations are conducted for a  $4 \times 4 \times 1$  supercell with a  $1 \times 1 \times 2$  k-mesh and an energy convergence criterion of  $10^{-5}$  eV. Note that the  $\Gamma$ -only AIMD simulation cannot reproduce correctly the interlayer distance of BN.

To ensure the AIMD simulations correctly capture the thermal expansion contribution, the pressure of the micro canonical (NVE) ensemble must be zero. In this work, the lattice constants are adjusted until the pressures of the NVE simulations reach zero at each different temperature. The time step in the simulation is set to 0.5 fs, which is short enough to resolve all the phonon modes in BN. Before each NVE simulation, isothermal-isobaric ensembles (NPT) simulations were conducted to equilibrate the system. The total NVE simulation time at each temperature is 40,000 steps with the first 5,000 steps discarded as the initialization steps and the remaining 35,000 steps are taken as the MD trajectory for the spectral energy density (SED) analysis [7, 8]. As shown in Fig. 1(a), the obtained SED for each phonon mode is a distinct peak, from which the anharmonic phonon energy can be extracted.

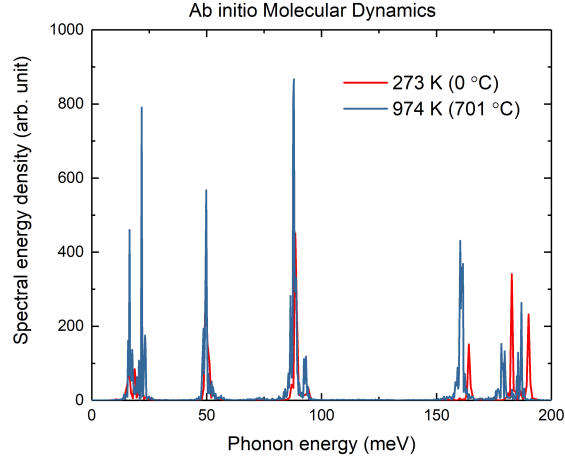
The anharmonic phonon scattering as a function of temperature, shown in the inset of Fig. 3a of the main manuscript, were obtained by calculating the difference between the AIMD phonon energy shift and the thermal expansion quasiharmonic shift contribution. The thermal expansion coefficients were calculated using the method developed in Ref. [9], which begins by first obtaining the harmonic phonon dispersions at different lattice constants as shown in Fig. 1(b). This allows to obtain the phonon energy dependence and pressure dependence on the lattice constant  $\partial E/\partial a$  and  $\partial P/\partial a$ , respectively, which then can be used to calculate the linear thermal expansion coefficient,  $1/a\partial a/T$ , from thermodynamical relations.

---

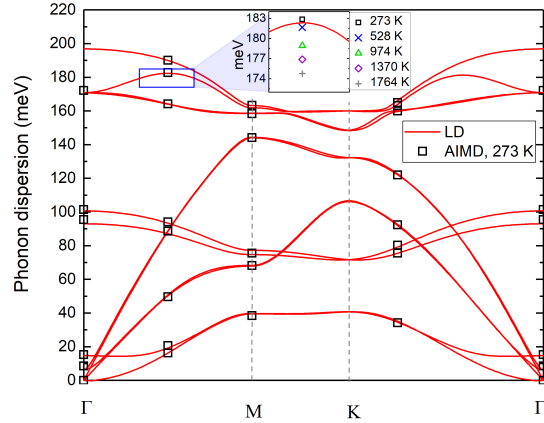
\* [idrobojc@ornl.gov](mailto:idrobojc@ornl.gov)

† [arl1000@ornl.gov](mailto:arl1000@ornl.gov)

[1] O.L. Krivanek, T.C. Lovejoy, N. Dellby, and R.W. Carpenter, *Microscopy* **62**, 3 (2013).



(a)



(b)

FIG. 1. Phonon spectral energy density (SED) and dispersion. (a) The phonon SED at  $q = (0.25, 0, 0)$  ( $\Gamma$ -M) extracted from ab initio molecular dynamics (AIMD) simulations at 273 K and 974 K. (b) The phonon dispersion calculated within linear dynamics (LD). The phonon energies extracted from AIMD accurately reproduce the phonon dispersion obtained with LD. The inset shows the energy shift of the optical phonon calculated with AIMD as the temperature increases. The AIMD calculated phonon energies shown in the inset are also plotted in Fig. 4a.

- [2] G. Kresse, *et al.*, Phys. Rev. B **47**, 558, (1993).
- [3] G. Kresse, *et al.*, Phys. Rev. B **54**, 11169, (1996).
- [4] G. Kresse, *et al.*, Comput. Mat. Sci. **6**, 15, (1996).
- [5] G.J. Exarhos, and J.W. Schaaf, J. Appl. Phys. **69**, 2543 (1991).
- [6] A. Togo, and I. Tanaka, Scr. Mater. **108**, 1 (2015).

- [7] N. de Koker, Phys. Rev. Lett. **103**, 125902, (2009).
- [8] T.L. Feng, and X.L. Ruan, J. Appl. Phys. **117**, 195102 (2015).
- [9] U. Argaman, E. Edelstein, O. Levy, and G. Makov, Phys. Rev. B **94**, 174305 (2016).